Buspirone Analogues as Ligands of the 5-HT$_{1A}$ Receptor. 1. The Molecular Structure of Buspirone and Its Two Analogues

Zdzisław Chilmonczyk,*,† Andrzej Leś,‡ Agnieszka Woźniakowska,† Jacek Cybulski,† Anna E. Kozioł,⊥ and Maria Gdaniec§

Pharmaceutical Research Institute, 8 Rydygiera Street, 01-793 Warszawa, Poland, Department of Chemistry, University of Warsaw, 1 Pasteur Street, 02-093 Warszawa, Poland, Department of Chemistry, Maria Curie-Skłodowska University, 3 Maria Curie-Skłodowska Square, 20-031 Lublin, Poland, and Department of Chemistry, Adam Mickiewicz University, 6 Grunwaldzka Street, 60-780 Poznań, Poland

Received July 22, 1994®

An interdisciplinary (X-ray, ^{1}H and ^{13}C NMR, IR, and theoretical quantum mechanical) study on the potent 5-HT$_{1A}$ receptor ligand buspirone (**1**) and its two structural analogues, mesmar (4,4-dimethyl-1-[4-[4-(2-quinolinyl)-1-piperazinyl]butyl]-2,6-piperidinedione) (**2**) and kaspar (8-[4-[4-(2-quinolinyl)-1-piperazinyl]butyl]-8-azaspiro[4.5]decane-7,9-dione) (**3**), has been reported. The results have shown that buspirone-like molecules should appear in an extended rod-shape form, possessing several potential interaction sites with the receptor.

Introduction

Pharmacological Response of Buspirone Analogues. N-Substituted arylpiperazines produce many of the behavioral responses and pharmacological effects stemming directly from the activation of the central serotonin system.[1-4] They also inhibit spontaneous firing of neurons in the dorsal raphe nucleus.[5] As a class they find wide use for the treatment of anxiety and depression.[6] Their antidepressant and anxiolytic activity has been confirmed by clinical evidence.[7] Apart from buspirone (**1**; Chart 1), which is the only approved non-benzodiazepine anxiolytic drug, there is its close structural homologue, ipsapirone (**4**).[7] This compound, which is presently clinically tested, has aroused considerable interest owing to its greater receptor specificity. Buspirone (**1**) and many structurally related compounds[8] suffer from poor bioavailability[9] and a delayed onset of efficacy of approximately 2 weeks.[10] Yet in spite of that, buspirone (**1**) is reported to be equally effective as benzodiazepine diazepam after 4 weeks of treatment.[10]

Theory of Buspirone's Anxiolytic Activity. In the central nervous system, the action of buspirone (1) as an anxiolytic is believed to proceed by way of binding to the 5-HT$_{1A}$ subtype of the serotonin receptors. In order to understand the molecular mechanism of buspirone (**1**) activity, it is necessary to determine the physicochemical factors that affect recognition and binding of buspirone (**1**) to the receptor. It is generally accepted that there are at least two structural features necessary for the recognition of ligands by the 5-HT$_{1A}$ receptor site.[11-13] One of these is the presence of an aromatic ring. The other is the basic nitrogen atom located at a distance of 5.2–5.7 Å from the aromatic ring center. Both structural units are present in the buspirone molecule. Hibert *et al.*[11,12] have described the pharmacophore for agonist and antagonist binding sites on the basis of the structural differences. In the agonists, the out-of-plane deviation of the basic nitrogen atom should have the value of 0.2 Å, while in the antagonists, it should be considerably larger, about 1.6 Å. This pharmacophore model was later supported by Agarwal and Taylor[14] who suggested, on the basis of results of the comparative molecular field analysis (CoMFA) implemented in the 3-D QSAR (SYBYL), that the agonists tend to be "flatter" (more coplanar) than the antagonists. The aromatic site and the NH$^+$ unit are essential building blocks of a pharmacophore model for 5-HT$_{1A}$ agonists and partial agonists recently formulated by Hackell *et al.*[15,16] Their pharmacophore was obtained in the course of molecular fitting and volume manipulation in a series of analogues structurally related to 2-aminotetralin. The relative positions (distances and orientation in space) of the aromatic site and the NH$^+$ unit were described by means of a presumed dummy atom and conical spacial regions. By selecting certain classes of relative positions of aromatic and NH$^+$

Chart 1. Chemical Formulas of Buspirone (**1**), Mesmar (**2**), Kaspar (**3**), and Ipsapirone (**4**)

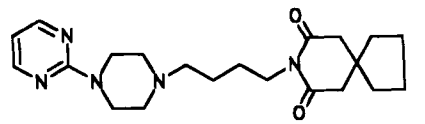

1

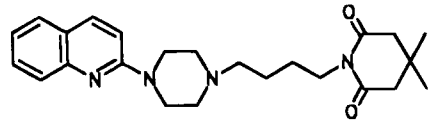

2

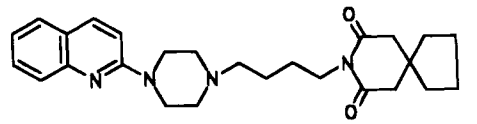

3

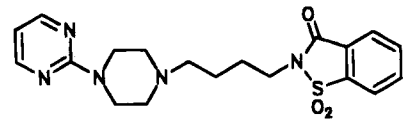

4

† Pharmaceutical Research Institute.
‡ University of Warsaw.
§ Adam Mickiewicz University.
⊥ Maria Curie-Sklodowska University.
® Abstract published in *Advance ACS Abstracts*, April 15, 1995.

0022-2623/95/1838-1701$09.00/0

Table 1. Affinities of Buspirone (1), Mesmar (2), Kaspar (3), and Ipsapirone (4) to the $5HT_{1A}$ Receptor[20a]

entry	compound	K_i (nM)
1	8-OH-DPAT (8)	1.44 ± 0.18
2	buspirone (1)	13.80 ± 1.60[a]
3	mesmar (2)	10.46 ± 1.70
4	kaspar (3)	38.60 ± 6.94
5	ipsapirone (4)	3.40 ± 0.98

[a] Reference 20b, K_i = 15 nM.

moieties, it was possible to define 3D models for potent and moderately potent 5-HT_{1A} agonists. Most of the structural characteristics described above can be found in buspirone (1), and it has been shown that buspirone exhibited properties of a partial agonist and antagonist of the 5-HT_{1A} receptors in different functional assays.[17]

Search for New Chemical Structures. The search to find new chemical structures with specific action upon central neurotransmission is a fast growing field of research.[18] In our laboratory we synthesized several new analogues of buspirone[19] showing high (nanomolar) affinity to the 5-HT_{1A} receptor. In this paper we report an interdisciplinary study on buspirone and its two analogues, mesmar (4,4-dimethyl-1-[4-[4-(2-quinolinyl)-1-piperazinyl]-butyl]-2,6-piperidinedione) (2) and kaspar (8-[4-[4-(2-quinolinyl)-1-piperazinyl]butyl]-8-azaspiro-[4.5]decane-7,9-dione) (3) (Chart 1). The investigations were carried out by X-ray and ^1H and ^{13}C NMR techniques and also theoretical quantum mechanical calculations. It should be noted that the present study reports the buspirone and buspirone hydrochloride molecular structures in three different environments. In the solid state, the buspirone molecules are surrounded by a strong crystal field originating from polar vicinal molecules. In the ^1H and ^{13}C NMR experiments, buspirone was dissolved in a weakly polar $CDCl_3$ solvent. The buspirone molecular structure in vacuum (no interactions with the environment) was predicted with the use of the theoretical quantum mechanical calculations.

The compounds studied are characterized by a significant pharmacological activity measured by the inhibitor affinity constant K_i (Table 1). Our aim was to determine the molecular structure and conformational flexibility of three potent 5-HT_{1A} ligands in order to better understand the molecular mechanism of their action during the first stages of interaction with the receptor. We also attempted to determine the possible pharmacophore related to the anxiolytic activity of buspirone analogues. We chose the solid-state conformations as starting data for molecular modeling. Therefore X-ray analyses for buspirone (1), mesmar (2), and kaspar (3) monohydrochlorides were performed. (The crystal structure of buspirone hydrochloride (1a) was determined by Yevich *et al.*,[21] but the atomic coordinates were missing in that paper. Neither could we find them in the Cambridge Structural Database.[22] Therefore in the present work, a new set of X-ray diffraction data was collected and the structure was redetermined.)

Methods

Crystallography. X-ray Crystal Structure Analysis. The crystals suitable for studies were obtained by recrystallization from an ethanol solution. For all crystal structure determinations, the single-crystal diffraction data were measured at room temperature on a KM4 diffractometer.[23] The intensities were corrected for Lorentz and polarization effects. The structures were solved by direct methods[24] and refined with anisotropic thermal parameters. A summary of the crystal data and structure refinements[25] is given in Table 2.

^1H and ^{13}C NMR Data. ^1H NMR spectra in $CDCl_3$ and NOE experiments were recorded on a Bruker AM 500 NMR spectrometer. ^{13}C NMR, COSY, and HETCOR spectra in $CDCl_3$ were obtained on a Bruker AC 200F instrument. Tetramethylsilane (TMS) was used as internal standard.

Computational Quantum Chemistry. We used the quantum chemical semiempirical AM1 method[26] and *ab initio* restricted Hartree–Fock (RHF) methods with standard atomic Gaussian basis sets implemented in the Gaussian 90 and Gaussian 92 codes[27] and installed on an IBM RISC 6000 workstation. We determined the molecular total energies, *i.e.*, the sums of electronic energy, and the repulsion of nuclei of buspirone and its structural analogues, as well as of several model compounds. The search for the energy-optimal molecular structures was carried out in two steps. In the first step, we performed the structure optimization by means of the AM1 method and then, for model compounds only, by the RHF method with the standard 3-21G, 6-31G*, 6-31G*(5d), or 6-31G** basis sets. In the next step we performed AM1 and RHF calculations of the harmonic vibrational frequencies and molecular electrostatic potentials (MEP's).

Results

Crystal Structures. The crystals of mesmar (2) and kaspar (3) hydrochlorides are isostructural (Table 2, Figure 1). Their structure consists of layers of molecules parallel to the *yz* plane. The arrangement of molecules makes possible only weak van der Waals interactions between hydrophobic quinoline and imide fragments, both within each layer and between layers. The van der Waals interactions of the terminal hydrophobic fragment of the kaspar (3) cation with the neighboring molecules contribute to the conformational disorder; the cyclopentane ring C25 atom (Figure 2) is disordered between two positions having site occupation factors of 0.22(2) and 0.88(2) which could be the result of the O2···H-C(25i) intermolecular hydrogen bonding. In the crystal structure of buspirone (1) hydrochloride, a different relative orientation of cations is observed (Figure 1) due to the presence of a pyrimidine ring instead of a quinoline one. The imide part of one cation is moved toward the *n*-butyl chain of surrounding cations. The crystal structures of the three hydrochlorides are built up of cation–anion pairs. The linear N^+-H···Cl^- hydrogen bond is observed within each structural unit (Table 3d).

Conformation of Cations in the Solid State. Bond lengths of the cations (Table 3a) are similar within the experimental error (2σ). The buspirone (1), mesmar (2), and kaspar (3) cations (Figure 2) have similar orientation of the piperazine ring *N*-substituents: both the aromatic ring at the N2 atom and the butyl chain at the protonated N3 nitrogen atom are placed in the equatorial position. The piperazine ring adopts the chair conformation.

The superposition of the molecular structures (Figure 3) and the similar values of the torsion angles (Table 3b) show that there are only small differences between the molecular geometry of mesmar (2) and kaspar (3). The most significant conformational changes are observed within the *n*-butyl spacer when the geometry of buspirone (1) is compared with that of mesmar (2) and kaspar (3). The *n*-butyl chain of buspirone adopts the *trans,trans,trans* conformation with only one torsion angle differing by −10° from the ideal 180° for the fully extended form. The *n*-butyl conformation in mesmar

Table 2. Crystal Data and Summary of X-ray Data Collection and Refinement Parameters of Buspirone (1), Mesmar (2), and Kaspar (3) Hydrochloride Structures

	buspirone	kaspar	mesmar
empirical formula	$C_{21}H_{31}N_5O_2 \cdot HCl$	$C_{26}H_{34}N_4O_2 \cdot HCl$	$C_{24}H_{32}N_4O_2 \cdot HCl$
formula weight	422.0	471.0	444.99
crystal system	monoclinic	monoclinic	monoclinic
space group	$P2_1/n$	$P2_1/c$	$P2_1/c$
unit cell dimensions			
a (Å)	14.747(3)	18.232(4)	17.741(4)
b (Å)	7.101(1)	11.230(2)	11.156(3)
c (Å)	21.536(4)	12.343(2)	12.277(3)
β (Å)	103.79(3)	91.95(3)	93.78(2)
V (Å^3)	2190.2(7)	2525.7(8)	2424.6(10)
Z	4	4	4
calcd density (g cm^{-3})	1.28	1.239	1.219
absorption coeff (mm^{-1})	0.198	0.177	0.184
F(000)	904	1008	952
	Data Collection (Mo Kα radiation, λ = 0.71069 Å)		
crystal size (mm)	0.2 × 0.3 × 0.1	0.5 × 0.5 × 0.1	0.6 × 0.6 × 0.1
2θ range (deg)	2.0−45.0	4.0−52.0	2.3−56.1
std refltns	2 measured every 50 refltns	2 measured every 100 refltns	2 measured every 100 refltns
std refltn variations (%)	<4	<3	<3.2
index ranges	$0 \le h \le 10$; $0 \le k \le 7$; $-23 \le l \le 22$	$0 \le h \le 22$; $-13 \le k \le 0$; $-15 \le l \le 15$	$0 \le h \le 23$; $-14 \le k \le 0$; $-15 \le l \le 15$
reflts collected	2026	5426	6037
independent (R_{int})	1775 (2.92%)	4995 (2.0%)	5867 (2.75%)
used in calcn	1204; $F_o \ge 3\sigma(F_o)$	2795; $F_o \ge 3\sigma(F_o)$	3165; $F_o \ge 4\sigma(F_o)$
	Solution and Refinement		
programs used	SHELXS-86, SHELXTL	SHELXS-86, SHELXTL	SHELXS-86, SHELXL-93
refinement method	full-matrix least-squares on F	block-diagonal least-squares of F	full-matrix least-squares on F^2
function minimized		$\sum w(\|F_o\| - \|F_c\|)^2$	$\sum w(F_o^2 - F_c^2)^2$
weighting scheme [w^{-1}]		$\sigma^2(F_o) + 0.0002F_o^2$	$\sigma^2(F_o^2) + (0.0921P)^2$; $P = 1/3[\max(F_o^2,0) + 2F_c^2]$
hydrogen atoms	riding model, U_{iso} refined	in ordered part: x, y, z, and U_{iso} refined	for all atoms: x, y, z, and U_{iso} refined
no. of parameters refined	264	419	412
final $R = \sum(\|F_o\| - \|F_c\|)/\sum(\|F_o\|$	0.0732	0.0573	0.0503
wR indices	0.0787	0.0632	0.1374; wR2 = $[\sum w(F_o^2 - F_c^2)^2/\sum w(F_o^2)^2]^{1/2}$
	$w\mathrm{R} = [\sum w(\|F_o\| - \|F_c\|)^2/\sum w\|F_o\|^2]^{1/2}$		
final wR indices for all refltns	0.0902	0.0828	0.1733
goodness-of-fit	2.09 (on F)	1.31 (on F)	0.973 (on F^2)
largest and mean Δ/σ	0.001, 0.00	0.099, 0.004 (max for disordered part)	0.789, 0.165 (max for H atoms)
residual difference peak (e Å^{-3})			
max	0.28	0.31	0.34
min.	−0.26	−0.36	−0.22

(**2**) and kaspar (**3**) is different at the central C16−C17 carbon−carbon bond and becomes *trans,(+)-gauche,-trans*. The conformational changes could result from different crystal packing. In the crystal structure of buspirone (**1**), the dominating interactions between cations are the O···C(H) contacts.

Theoretical Quantum Mechanical Calculations. Minimum Energy Structures. The crystallographic data indicate that buspirone (**1**), mesmar (**2**), and kaspar (**3**) appear in the solid state in extended (not folded) conformations (Figure 3). This, in turn, suggests that those extended conformations belong to a set of the most energetically stable structures and probably appear in the liquid state as well. In the present work we performed a search for minimum energy structures of buspirone (**1**), mesmar (**2**), kaspar (**3**), and their hydrochlorides by the semiempirical AM1 method. The calculations have shown that the theoretical structures correspond to the extended rod-shape form of the molecules. Essentially similar molecular structures obtained for protonated and not protonated species might suggest that the molecules should remain in their extended forms even in a strongly polar environment.

Conformational Flexibility. α-, β-, and φ-Angle Variation in Buspirone (1) and Mesmar (2). The conformations adopted in gas and liquid phases by the molecules possessing several C−C and C−N single bonds can in general be different from those found in the solid state. In order to explore the conformational flexibility of a parent compound (buspirone, **1**), we performed the calculations of the conformational energy map. A set of conformations was obtained with the use of the rotations of respective molecular fragments around three bonds denoted as α, β, and ϕ (Figure 3, Table 3). Each conformation was characterized by the total molecular energy $E(\alpha,\beta,\phi)$ and the value of the density of probability $Z(\alpha,\beta,\phi)$:[28]

$$Z(\alpha,\beta,\phi) = Z_0 e^{-E(\alpha,\beta,\phi)/kT}$$

where k is the Boltzmann constant, T is the temperature (T = 298.15 K), and Z_0 is the normalization factor. The minimum energy conformation was found to correspond to $\alpha_0 = 17.8°$, $\beta_0 = 70.3°$, and $\phi_0 = 87.1°$. The molecular total energies $E(\alpha,\beta,\phi)$ were subsequently calculated for

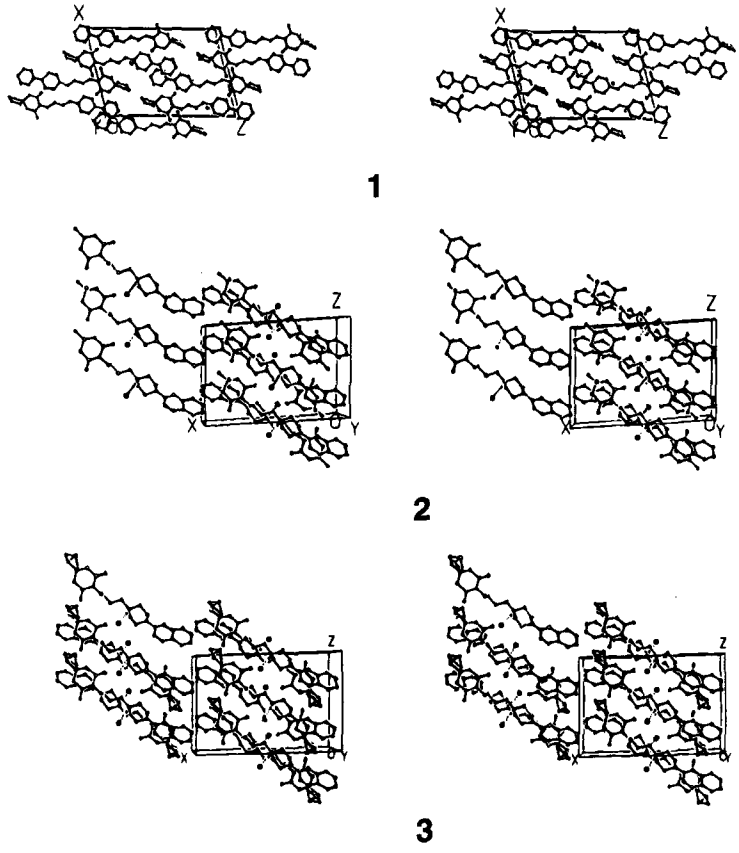

Figure 1. Stereoview of crystal packing in the buspirone (**1**), mesmar (**2**), and kaspar (**3**) hydrochloride crystal structures (down the *y* axis).

a grid of angles with the $\Delta\psi = 6°$ scanning, *i.e.*, $E(i,j,k) = E[(\alpha + i\Delta\psi),(\beta + j\Delta\psi),(\phi + k\Delta\psi)]$ and $i, j, k = 0, 1, \ldots 6$. The minimum energy was $E(\alpha_0,\beta_0,\phi_0) = -0.0559$ hartree. On the basis of the calculated *Z*-values, we determined several regions on α,β,ϕ space corresponding to the highest density of probability of stable conformations. It appeared that the regions of relatively large *Z*-values are very narrow, thus indicating that buspirone (1) is characterized by a rather stiff molecular structure. A rotation around the α-bond seems to be unfavorable (barrier height of 30.9 kJ mol^{-1}). (The corresponding barrier height for 1-(2-pyrimidyl)piperazine (**5**) (the model of the buspirone aromatic part) calculated with the aid of *ab initio* RHF/3-21G method is 66.9 kJ mol^{-1}.) The "softest" rotation corresponds to the β-bond (barrier height of 14.2 kJ mol^{-1}). It should be noted that no conformations were found more stable than the fully extended form. The rotation about the α-bond was also studied by freezing all the remaining geometrical parameters. It appeared that the overall shapes of the $E(\alpha)$ energy profiles in buspirone (**1**) and mesmar (**2**) seemed to be similar. Quantitatively one can compare the two energy profiles of molecules A and B making use of the conformation similarity index recently defined by Baginski and Piela:[29]

$$K_{A,B} = 1 - {}^1/_2\int |Z_A(\phi) - Z_B(\phi)|\, d\phi$$

where ϕ is the rotation angle in the A and B molecules and *Z* is the probability density function defined above. The values of the $K_{A,B}$ index belong to the (0,1) interval. The calculated value of $K_{A,B} = 0.68$ (A, buspirone; B, mesmar) suggests considerable similarity between α-rotations in buspirone and mesmar.

δ-Angle Variation in *n*-Butyl Spacer of Buspirone. The rotation about the single C–C bonds in the butyl moiety of buspirone (**1**) can provide a variety of conformations which are characterized by similar total energy values. In order to determine the flexibility of butyl moiety conformations, we calculated the molecular energy changes scanning the central δ-angle (rotation around C16–C17) with the $\Delta\delta = 15°$ step (with neighboring bonds frozen). We found that a δ-rotation of $\delta = \pm 45°$ led via a little energy barrier of some 6.3 kJ mol^{-1} to other shallow energy minima located 3.3 kJ mol^{-1} above the reference energy corresponding to $\delta = 180°$. Further δ-rotation was considerably hindered (barrier height of about 40 kJ mol^{-1}). These observations suggest that the butyl spacer undergoes a wagging movement which provides the majority of *all-trans* conformations perturbed by a fraction of *trans,gauche* conformations. The calculated high rotational barrier for the representative δ-bond rotation is a first indication that the many dimensional conformational space can be significantly reduced to narrow regions, most probably covering those conformations which are close to the extended zigzag forms. In general, the minimum energy structures resulting from the calculations based on the semiempirical AM1 method are in agreement with those found in the solid state. For the compounds studied, the fully extended conformation appeared to be most favorable.

The validity of the AM1 method in predicting molecular structures related to buspirone (**1**) was assessed on the model compound 1-(2-pyrimidyl)piperazine (**5**) by

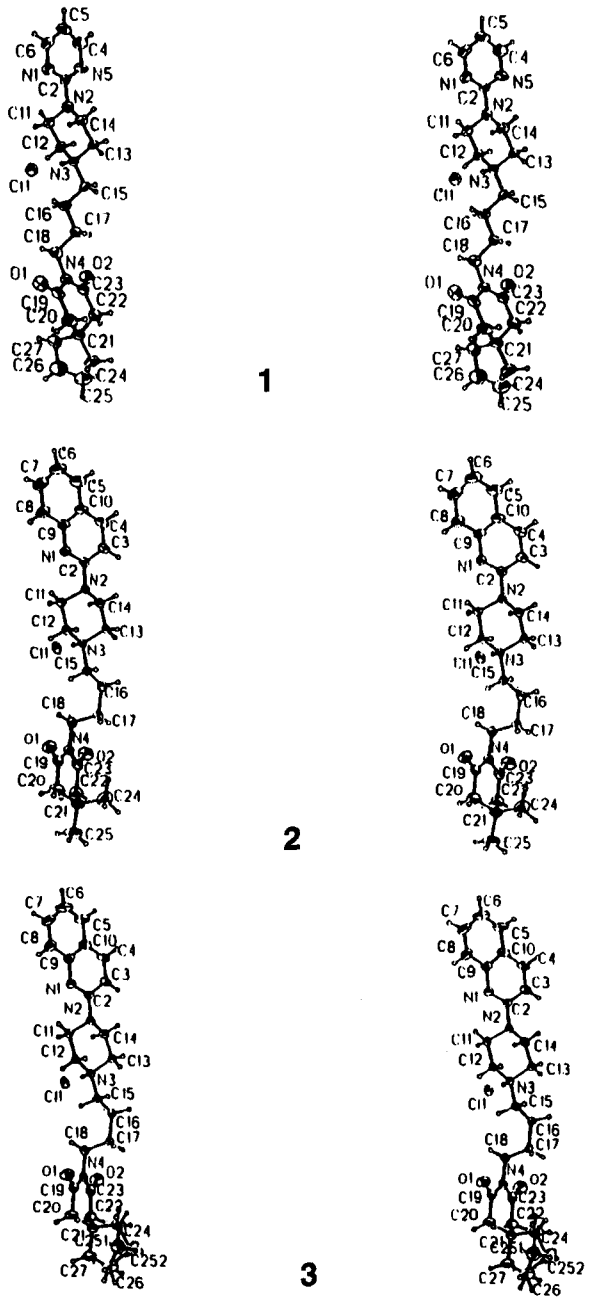

Figure 2. Stereoscopic view and atom labeling of the buspirone (1), mesmar (2), and kaspar (3) hydrochloride molecules.

the *ab initio* SCF/6-31G* method. The results (see Table 7 in the supplementary material) suggest that molecular geometries obtained with the AM1 method are reasonable. For the *n*-butyl spacer, the quantum mechanical AM1 calculations predicted the *all-trans* conformation. Small structural differences were found in the *n*-butyl spacer conformation in the solid state of mesmar (2) and kaspar (3).

Dipole Moment of Buspirone (1), Buspirone H^+ Cation, and Buspirone Hydrochloride. We observed dramatic changes in electron cloud distribution following the protonation of the piperazine nitrogen atom. For neutral (not protonated) buspirone, the electric dipole moment of 3.5 D is colinear with the N(piperazine)–C(butyl) bond. Upon protonation of the nitrogen atom (in buspirone H^+ cation), the dipole moment increases up to 10.5 D and rotates by some 160°. In buspirone hydrochloride, where the hydrochloride molecule faces the basic N3 nitrogen atom, the dipole moment becomes equal to 5.8 D and deviates by 38° from the N3–C4 direction. A dipole moment increase was also seen in mesmar (2) and kaspar (3) hydrochlorides from 4.5 up to 5.1 D and from 4.6 up to 5.5 D, respectively. Such significant changes in electronic cloud distribution suggest the appearance of strong orientational effects upon protonation/deprotonation of the basic nitrogen atom. These effects may contribute to the buspirone analogues recognition at the first stages of interaction with the receptor and also during the release from the active site.

Molecular Electrostatic Potential. The buspirone molecule is characterized by several polar groups or moieties that can strongly interact with the receptor. The NH^+ moiety constitutes the primary interaction site with the receptor. Moreover, there exist other regions of the molecule that should be taken into account. These are the nitrogen atoms of the pyrimidine ring and the two carbonyl groups of the imide moiety. The interaction sites can be conveniently characterized with the aid of the molecular electrostatic potential (MEP).

Table 3. Structural Parameters[a]

(a) Selected Bond Distances (Å)

	buspirone (1)	mesmar (2)	kaspar (3)
N1–C2	1.33(2)	1.311(3)	1.320(5)
C2–N2	1.39(2)	1.393(3)	1.387(4)
N2–C2	1.46(1)	1.454(3)	1.465(5)
N2–C14	1.44(2)	1.449(3)	1.446(5)
C11–C12	1.48(1)	1.503(3)	1.504(5)
C13–C14	1.51(1)	1.487(3)	1.502(5)
C12–N3	1.49(1)	1.490(2)	1.486(4)
N3–C13	1.49(1)	1.488(2)	1.486(4)
N3–C15	1.51(1)	1.493(3)	1.496(4)
C15–C16	1.50(1)	1.509(3)	1.522(5)
C16–C17	1.49(1)	1.523(3)	1.524(5)
C17–C18	1.52(1)	1.518(3)	1.524(5)
C18–N4	1.48(1)	1.473(3)	1.467(5)
N4–C19	1.39(2)	1.387(3)	1.380(5)
C19–C20	1.49(2)	1.498(4)	1.499(6)
N4–C23	1.40(3)	1.395(3)	1.395(5)
O1–C19	1.23(2)	1.202(3)	1.207(5)
O2–C23	1.20(1)	1.204(3)	1.206(5)
C22–C23	1.47(2)	1.498(4)	1.485(6)

(b) Torsion Angles (Deg)

	buspirone		mesmar	kaspar
	(theoretical)	(crystal)	(crystal)	(crystal)
C11–N2–C2–N1 (α)	17.8	12.0(4)	19.6(3)	20.7(4)
C12–N3–C15–C16 (β)	70.3	73.7(4)	177.4(2)	177.4(3)
N3–C15–C16–C17 (γ)	180.0	174.5(3)	−159.4(2)	−157.9(3)
C15–C16–C17–C18 (δ)	180.0	−169.4(3)	76.1(3)	74.0(4)
C16–C17–C18–N4 (ε)	180.0	−177.0(4)	177.5(2)	174.9(4)
C17–C18–N4–C19 (φ)	−88.7	113.2(5)	91.1(3)	94.2(5)

(c) Intermolecular Distances (Å)

	buspirone		mesmar	kaspar
	(theoretical)	(crystal)	(crystal)	(crystal)
$N^+3\cdots N4$	6.27	6.30	5.71	5.68
center of heterocyclic ring$\cdots N^+3$	5.64	5.51	5.61	5.61
deviation of N^+3 from the heterocyclic ring plane	0.38	0.36	0.26	0.19

(d) Hydrogen-Bond Geometry in the Crystal Structure

	$N^+3\cdots Cl$ (Å)	N^+3–H3 (Å)	H3$\cdots$Cl (Å)	N^+3–H3$\cdots$Cl (deg)
buspirone	3.102(12)	0.90	2.21	175
mesmar	3.028(2)	0.92(3)	2.11(3)	174(2)
kaspar	3.015(4)	0.92(4)	2.10(4)	178(3)

[a] N^+3 denotes the protonated nitrogen atom.

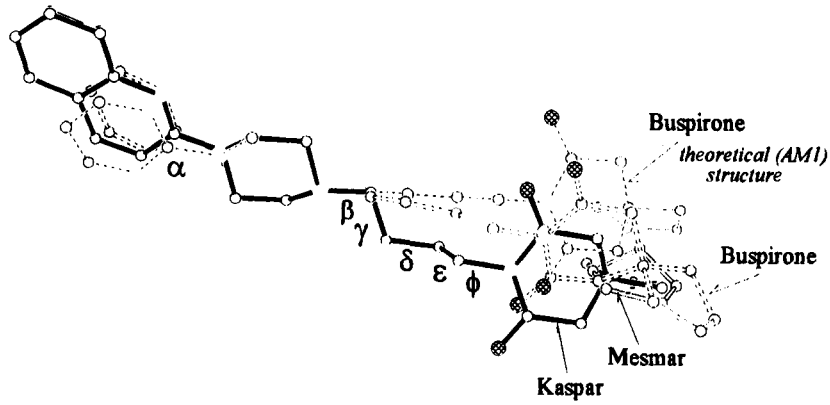

Figure 3. Superposition of 1–3 cation structures and the theoretical (AM1) conformation of buspirone (1).

The MEP values can also be instrumental in characterization of the Coulomb complementarity between the enzyme (proteins) and its ligands.[30,31] The MEP values at the space point $P(X,Y,Z)$ were calculated according to the formula:

$$\mathrm{MEP}(P) = \sum_{\mathrm{A}} \frac{Z_{\mathrm{A}}}{r_{AP}} - \int \frac{\varrho(i)}{r_{iP}}\, \mathrm{d}\tau_i$$

where Z_A is the charge of nucleus A distant by r_{AP} from the space point P and $\varrho(i)$ is the electronic density. The MEP values were calculated by the semiempirical AM1 method for certain space regions of buspirone (**1**) and some of the potent 5-HT_{1A} ligands such as LSD (**7**) and 8-OH-DPAT (**8**). The MEP values were also calculated for 1-(2-pyrimidyl)piperazine (**5**) (the buspirone aromatic part model) and 3,3-tetramethyleneglutarimide (**6**) (a model of the imide moiety in buspirone, mesmar, and kaspar) systems by the *ab initio* RHF/3-21G and RHF/6-31G*(5d) methods. The present theoretical calculations of the MEP values suggest that in the vicinity of the aromatic ring and the imide carbonyl groups there exist deep negative electric potential wells (Figure 5) that can be involved, via hydrogen bonds, in the docking process. The MEP's were calculated for a mesh of points belonging to the plane located 1.6 Å away from the molecular plane. The complicated MEP 3D hypersurface is schematically presented in Figure 4. It can be seen that two electric potential wells appear—one near the basic piperazine nitrogen (−171.4 kJ mol^{-1}) and the other near the pyrimidine nitrogen atoms (−110.8 kJ mol^{-1}). The former well can undergo rather fast protonation, while the latter, though much less deep, is still able to attract proton donor moieties of the receptor. A similar MEP well (of about −110 kJ mol^{-1}) appears in the vicinity of the carbonyl oxygen atoms in 3,3-tetramethyleneglutarimide (**6**). The calculated MEP values at the mesh located in the molecular plane show a rather deep (−222.0 kJ mol^{-1}) electric potential well particularly suited for strong hydrogen bonds with the receptor. (The discussed MEP values were also calculated with the use of the semiempirical quantum mechanical AM1 method. The qualitative picture of the MEP wells remains the same though the numerical values of AM1 MEP's become nearly twice as large as the *ab initio* values, *e.g.*, the AM1 MEP well in the vicinity of the pyrimidine nitrogen atom becomes as deep as −241.2 kM mol^{-1}. Such a large difference of the calculated MEP values reflects an approximate character of the AM1 method.) We also calculated the MEP wells (by the AM1 method) for other potent ligands of the 5-HT_{1A} receptor, *i.e.*, for LSD (**7**) and 8-OH-DPAT (**8**) in the neutral (not protonated forms), and compared the regions that potentially could be involved in the interaction with the receptor. For LSD (**7**) we found that at 1.6 Å above the molecular plane there exists a deep (−438.9 kJ mol^{-1}) electronegative potential in front of the carbonyl oxygen atom. The other two electric potential wells can be found in front of the basic nitrogen atom (−313.5 kJ mol^{-1}) and close to the indole ring (−213.2 kJ mol^{-1}) in front of the C9=C10 double bond. The latter MEP well was formerly identified by Weinstein *et al.*[32] in their pseudopotential minimal basis set LP-3G calculations. All three regions characterized by deep negative electric potential values can be involved in the recognition process of LSD by the 5-HT_{1A} receptor. Another potent 5-HT_{1A} ligand, the 8-OH-DPAT (**8**) molecule, also exhibits molecular regions that are characterized by deep electronegative potential wells. These regions can be found in the vicinity of a basic nitrogen atom (−263.3 kJ mol^{-1}) and close to the hydroxyl oxygen atom (−146.3 kJ mol^{-1}). Probably the most interesting features of the present calculations of MEP values are the relative values of MEP minima. In the compounds studied the primary interaction site appears to be the basic nitrogen atom, the next sites are probably the carbonyl oxygen atoms, and the relatively weakest interaction sites are nitrogen or oxygen atoms connected to the aromatic rings. The results suggest that the 8-OH-DPAT molecule can serve as a bidentate 5-HT_{1A} ligand. The primary interaction site is composed of a basic nitrogen atom. The secondary interaction point is located in the vicinity of the hydroxyl oxygen atom and close to the phenyl ring. The LSD molecule has probably three interaction points, *i.e.*, the basic nitrogen, the carbonyl atom, and the region close to the C9=C10 double bond. The buspirone (**1a**) (also mesmar, **1b**, and kaspar, **1c**) molecule can be characterized by even more (four) interaction sites.

^{1}H and ^{13}C NMR. The essential structural features of buspirone (**1**) hydrochloride deduced from the X-ray studies in the solid state (strong intermolecular interactions with the environment) and from the theoretical quantum mechanical calculations (no interactions with the environment) are similar. Thus, we can expect that in weakly polar $CDCl_3$ solutions most of the buspirone hydrochloride structural units appear in forms similar to those found in crystals and predicted for vacuum.

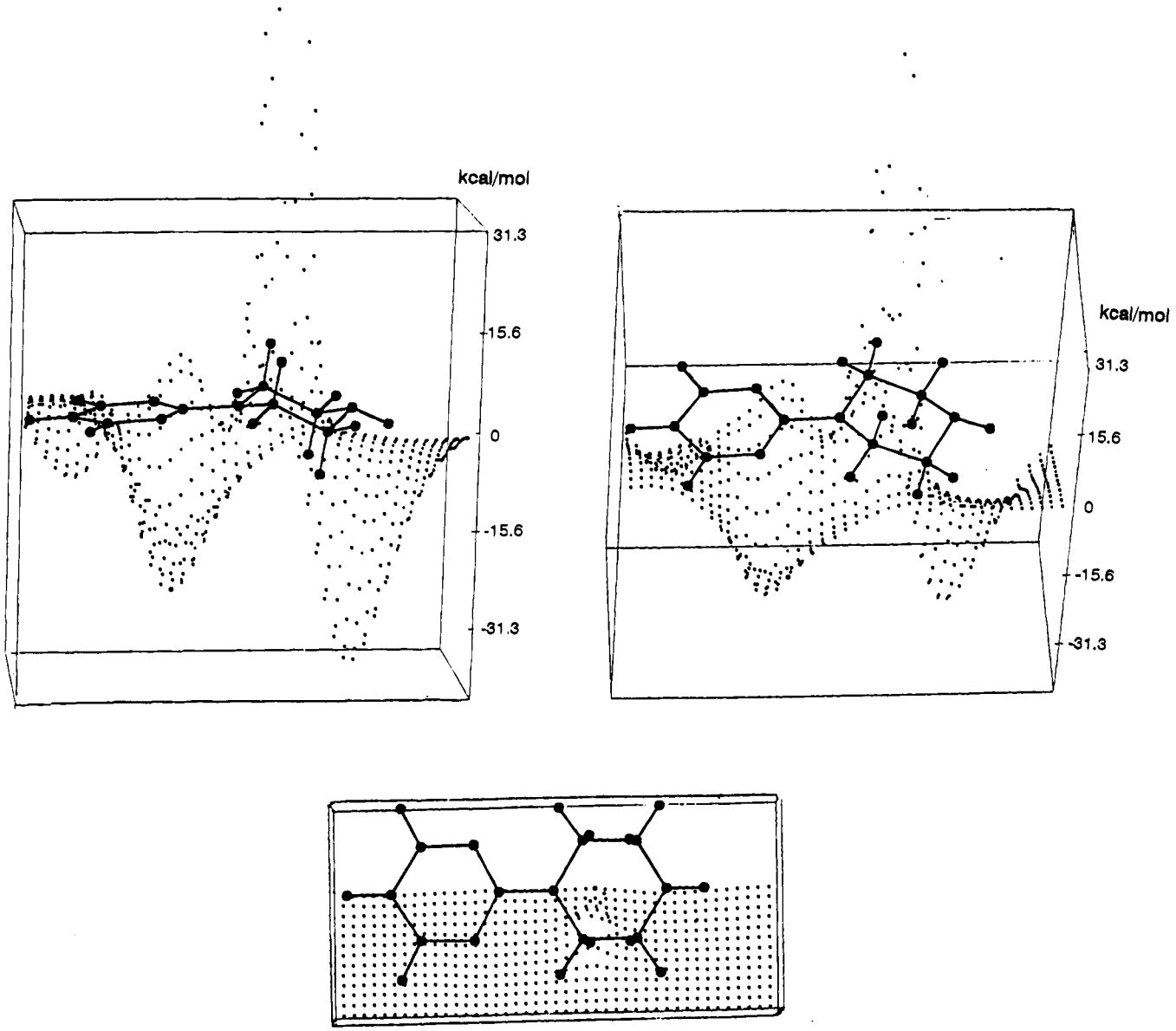

Figure 4. Molecular electrostatic potential (MEP) of 1-(2-pyrimidyl)piperazine (**5**). The MEP values (vertical axis, kcal mol^{-1}) were calculated with the use of the *ab initio* RHF/6-31G** method for a mesh of points (*P*, see text) belonging to the plane located 1.6 Å away from the pyrimidine ring plane. The MEP surface is seen from the top (lower panel), middle (right panel), and horizontal (left panel) view points. Due to the C_S symmetry of 1-(2-pyrimidyl)piperazine, only one-half of the MEP surface was visualized.

In the conventional one-dimensional ^{13}C NMR and DEPT spectrum, the low-field signals belong to the molecular fragments located at the opposite sites of the buspirone (**1**) molecule: $\delta = 172.43$ ppm represents the imide C19 and C23 (Figure 2) carbon atoms, $\delta = 160.78$ ppm corresponds to the pyrimidine C2 atom, $\delta = 157.92$ ppm originates from C4 and C6 (pyrimidine ring), and $\delta = 111.42$ ppm is assigned to C5 (pyrimidine ring). On the basis of the data reported for spirodecanes,[33] we assigned the following signals to carbon atoms: $\delta = 44.75$ ppm to C20 and C22, $\delta = 39.46$ ppm to C21 (spiro carbon atom), $\delta = 37.55$ ppm to C24 and C27, and $\delta = 24.15$ ppm to C25 and C26. The assignment of the bands corresponding to the aliphatic carbon atoms becomes more difficult. A comparative analysis of the ^{13}C NMR spectrum of the free base of buspirone and its hydrochloride form furnished information concerning the signals originating from carbon atoms placed in the α-, β-, and γ-positions with respect to the quaternary (assigned to N3) nitrogen atom. In the ^{1}H NMR spectrum, a definite assignment cannot be made on the basis of chemical shifts only. The proton–proton coupling was used to elucidate the connectivity of the carbon atoms to which the protons are attached. Two-dimensional ^{1}H correlation spectroscopy (2D COSY) was employed in the assignment of signals corresponding to the protons connected with the piperazine and carbon atoms belonging to the aliphatic chain. In particular, the diprotonic doublet at $\delta = 4.84$ ppm represents the equatorial H11e and H14e protons ($J = 14.67$ Hz). A complex multiplet signal at $\delta = 3.85$ ppm was assigned to the axial H11a and H14a protons ($J = 14.63$ Hz). The heteronuclear proton–carbon correlation spectrum (2D HETCOR) was used in the assignment of the ^{1}H and ^{13}C NMR spectra of buspirone (**1**). On that basis the following signals were assigned, $\delta = 56.89$ ppm to C15 (the carbon atom from the aliphatic chain attached to the piperazine nitrogen atom), $\delta = 51.62$ ppm to C12

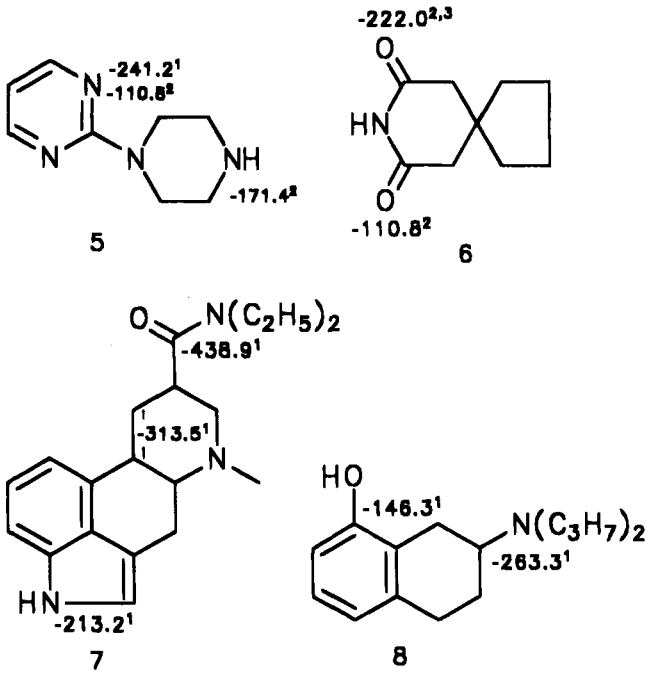

Figure 5. Molecular electrostatic potential wells (kJ mol^{-1}) for 1-(2-pyrimidyl)piperazine (**5**), 3,3-tetramethyleneglutarimide (**6**), LSD (**7**), and 8-OH-DPAT (**8**) at the plane located 1.6 Å from the molecular plane calculated with the use of the AM1 (1) and the *ab initio* RHF/6-31G*(5d) (2) methods. (3) Value calculated at the plane of the carbonyl groups.

and C13 (the piperazine ring), δ = 40.51 ppm to C11 and C14 (the piperazine ring), δ = 37.82 ppm to C18 (the carbon atom from the aliphatic chain attached to the imide fragment), δ = 25.02 ppm to C17 (the carbon atom from the aliphatic chain), and δ = 20.46 ppm to C16 (also the carbon atom from the aliphatic chain). After the assignment of all the carbon and proton signals, a NOE experiment on the hydrogen atoms connected to C18 (*n*-butyl carbon atom α to the imide nitrogen atom) was performed. The experiment has shown that the *n*-butyl spacer in buspirone $CDCl_3$ solution existed in a not folded conformation.

Molecular Structure of Buspirone-Like 5-HT_{1A} Ligands. The crystal structure and NMR spectra of buspirone (**1**) (and its structural analogues) hydrochloride have undoubtedly shown that the protonated nitrogen atom, constituting the primary interaction site, belongs to the piperazine ring (N3). In the buspirone–receptor complex, the protonated nitrogen is probably directed toward a hydrogen bond acceptor in the receptor protein chain. The second and third interaction sites of buspirone are located in the vicinity of the cyclic imide moiety in front of the carbonyl oxygen atoms. The first, second, and third interaction sites are characterized by a similar, deep MEP well of about −165 to −210 kJ mol^{-1}. Such large negative potential values suggest a possible formation of strong hydrogen bonds with the environment (NH, OH moieties of the receptor protein chain). These hydrogen bonds should be strong enough to orient the entire buspirone-like molecules in a way that is necessary to start the biotransformation. The fourth interaction site of buspirone (**1**), mesmar (**2**), and kaspar (**3**) is located in the vicinity of the aromatic ring in front of the endocyclic nitrogen atom. The present theoretical calculations (*ab initio* SCF and semiempirical AM1) show a deep MEP well of about −100 kJ mol^{-1}. The bottom of this MEP well corresponds to the electrostatic potential well in the vicinity of the phenolic oxygen in 8-OH-DPAT (**8**) and the double C9=C10 bond region of the LSD (**7**) skeleton. Weinstein *et al.*[31,32,34] have repeatedly pointed out the importance of this region in understanding the molecular mechanism of the action of the 5-HT_{1A} ligands.

Several building blocks of the buspirone (**1**) skeleton are characterized by their own conformational properties. The aromatic ring is rigid and planar. The piperazine ring is flexible. In the crystalline state the piperazine ring adopts exclusively the chair conformation. From the theoretical AM1 studies, it also appears that the chair conformation is stable, and it probably corresponds to the global energetic minimum. On the basis of the present ^1H NMR spectra, one cannot exclude a possibility that the piperazine ring undergoes a fast pseudorotational motion. The piperazine ring flexibility is similar to that found in cyclohexane, a structural analogue of piperazine. In cyclohexane there appear several conformations that are close to the minimum energy chair conformation.[35] The aromatic pyrimidine or quinolidine rings can be attached to the piperazine nitrogen in the equatorial or axial positions. These two positions generate different relative rearrangements of the aromatic and piperazine rings: the aromatic ring in the equatorial position will remain nearly coplanar with the piperazine ring, while the axial position turns both rings almost perpendicular in space. In the solid state only equatorial conformations of aromatic rings were found (deviation of the N3 nitrogen atom from the heteroaromatic ring plane in the range 0.2–0.4 Å). The rotation about the equatorial C(aromatic)–N(piperazine) bond is largely hindered, as suggested by the present theoretical quantum mechanical calculations (see the former section for buspirone model calculations).

In principle, the butyl spacer can be the most flexible structural building block of the entire buspirone skeleton due to a sequence of five single bonds, *i.e.*, N–(–C–C–C–C–)–N. Surprisingly, the conformational flexibility appears to be constrained to some extent. The spectra of buspirone have shown that the *n*-butyl spacer should appear in an extended form in a nonpolar solution. In the solid state, the *n*-butyl moiety of buspirone exists in the fully extended conformation (*trans,trans,trans*). The *n*-butyl conformations in the solid states of mesmar (**2**) and kaspar (**3**) are also extended but adopt *trans,(+)-gauche,trans* forms. Moreover, one can expect, on the basis of the theoretical AM1 calculations, that the butyl spacer should adopt conformations close to the extended zigzag forms, *i.e.*, a majority of conformations should not be folded or partly folded. The putative *n*-butyl moiety rotations should then be hindered to some extent. The cyclic imide has, in principle, no conformational degrees of freedom (except for the C25 carbon atom in the cyclopentane ring), and its special molecular structure should remain constant.

Discussion

In the present work we attempted to define the common structural features of the buspirone-like molecules in order to better understand the molecular mechanism of their pharmacological activity. Their

structural features consisting of molecular electrostatic potential wells, the basic nitrogen atom, and the extended *n*-butyl spacer constitute the basis for the 5-HT_{1A} pharmacophore description. The present model is similar to the pharmacophore defined by Hibert,[11] Agarwal and Taylor,[14] and also, to some extent, in the recent paper of Vallagarda *et al.*[16] There are, however, differences in the conformational preferences.

It is generally accepted that a pharmacophore should contain a group (a moiety) of atoms adopting rather fixed (rigid) spatial structure in order to perfectly dock into the receptor site (Marshal's "active analogue approach"[36]). A molecule with a flexible structure is less useful as a potential candidate for pharmacophore construction.[12] In our opinion, a rigid pharmacophore should rather be replaced by a more flexible unit that can better accommodate the complex van der Waals surface of the receptor polypeptide chain. The postulated conformational flexibility must be limited to some extent in order to preserve the agonistic properties. These conformational constraints are deduced from the molecular structure of potent 5-HT_{1A} ligands such as 8-OH-DPAT and LSD. The aromatic piperazine ring coplanarity is probably a key factor to differentiate between the agonistic and antagonistic properties of a series of buspirone analogues. The analogues with coplanar rings should possess the properties of the 5-HT_{1A} receptor agonists. The analogues with the aromatic ring placed perpendicularly with respect to the piperazine ring are the 5-HT_{1A} antagonists (*e.g.*, spiperone, pindolol, methiothepin).[11]

Many allowable conformations of the side chain can also enhance the antagonistic properties (pindolol). The conformation of the butyl spacer may thus play an important role in binding to the 5-HT_{1A} receptor site. According to Mokrosz *et al.*,[37] the hydrophobic interactions of the hydrocarbon chain with the receptor can significantly affect the ligand affinity. The conformational flexibility of the side chains should thus become a subject of further theoretical and experimental studies. For example, tryptophan, a 5-HT structural analogue, appears in only six well-defined rotameric structures, although in principle it could adopt an infinite number of different rotameric forms due to the presence of three single C-C bonds.[38] It is assumed on the basis of the structure of bacteriorhodopsin[39-41] that the receptor protein chain passes seven times through the membrane. Recent studies have shown that the buspirone (or other 5-HT_{1A} ligand) binding site is located inside the membrane being embedded by a sequence of some 30 polar amino acids.[42] It is proposed by Hibert *et al.*[43] in their models of protein G-coupled receptors that the α-helices surrounding the ligand-binding region are very tightly packed and form a narrow dihedral cleft. One can speculate that the active site could be a channel that is blocked at the exit. The extended conformation of Buspirone analogues may facilitate their approach to the active site in which the compounds may be trapped at the first stages of the ligand–receptor interaction. The orientational effects upon protonation/deprotonation of the basic nitrogen atom and hydrogen bond formation between a receptor site and molecular regions with relatively deep MEP wells should be strong enough to force the required conformational changes and orient all the buspirone-like molecules in a way that is necessary to start the biotransformation.

Conclusions

The present crystallographic, spectral ^1H and ^{13}C NMR, and quantum mechanical theoretical studies suggest that 5-HT_{1A} receptor ligands structurally related to buspirone (**1**) (as those studied in the present paper) should appear in the extended rodlike forms. These forms have similar relative positions of the aromatic ring and the basic nitrogen atom, resembling in this respect 8-OH-DPAT and LSD. All of these compounds are also characterized by regions of deep negatively charged molecular electrostatic potentials (two wells for 8-OH-DPAT, three wells for LSD, and four wells for buspirone-like compounds) that can serve as an interaction site with the receptor. As the pharmacological activity of these compounds differs significantly, we suggest that a simple Hibert model of the 5-HT_{1A} pharmacophore should be modified in order to include some other structural features related to global molecular dimensions (length, diameter, van der Waals envelope) and electron density distribution (electrostatic potential, electric field). These additional characteristics should help understand the recognition and docking of ligands, via intermolecular hydrogen bonds, to the 5-HT_{1A} receptor.

Acknowledgment. This study was supported by the Polish State Committee for Scientific Research (KBN) Grant No. 6 6378 92 03 (1992–1995).

Supplementary Material Available: Complete tables of crystallographic data, atom coordinates, anisotropic thermal parameters, bond lengths, angles, and intermolecular distances, parameters describing the theoretically predicted molecular structures of the discussed molecules, and 2D NMR spectra of buspirone (8 pages). Ordering information is given on any current masthead page.

References

(1) Maj, J.; Lewandowska, A. Central Serotoninmimetic Action of Phenylpiperazines. *Pol. J. Pharmacol. Pharm.* **1980**, *32*, 495–504.
(2) Simansky, K. J.; Schechter, L. E. Properties of Some 1-Arylpiperazines as Antagonists of Stereotyped Behaviors Mediated by Central Serotoninergic Receptors in Rodents. *J. Pharmacol. Exp. Ther.* **1988**, *247*, 1073–1081.
(3) Glennon, R. A.; Naiman, N. A.; Prieson, M. E.; Titeler, M.; Lyon, R. A.; Herndon, J. L. Stimulus Properties of Arylpiperazines: NAN-190, a Potential 5HT_{1A} Serotonin Antagonist. *Drug Dev. Res.* **1989**, *16*, 335–343.
(4) Tatarczyńska, E.; Pawłowski, L.; Chojnacka-Wójcik, E.; Maj, J. The Central Action of 1-(2-Pyrimidinyl)piperazine, an Ipsapirone Metabolite. *Pol. J. Pharmacol. Pharm.* **1989**, *41*, 51–61.
(5) Traber, J.; Glaser, T. 5HT_{1A} Receptor-Related Anxiolytics. *Trends Pharmacol. Sci.* **1987**, *8*, 432–437.
(6) Romero, A. G.; McCall, R. B. Advances in Central Serotoninergics. In *Advances in Medicinal Chemistry*; Bristol, J. A., Ed.; Academic Press: New York, 1991; Vol. 27, Chapter 3.
(7) Murphy, D. L.; Leach, K. P.; Aulakh, C. S.; Pigott, T. A., III. Serotonin-Selective Arylpiperazines with Neuroendocrine, Behavioral, Temperature and Cardiovascular Effects in Humans. *Pharmacol. Rev.* **1991**, *43*, 527–552.
(8) Hoyer, D.; Schoeffter P. 5-HT Receptors: Subtypes and Second Messengers. *J. Recept. Res.* **1991**, *11*, 197–214.
(9) Caccia, S.; Fong, M. H.; Garattini, S.; Notarnicola, A. Ionization Constants and Partition Coefficients of 1-Arylpiperazine Derivatives. *Biochem. Pharmacol.* **1985**, *35*, 393–394.
(10) Goa, K.; Ward, A. Buspirone - a Preliminary Review of its Pharmacological Properties and Therapeutic Efficacy as an Anxiolytic. *Drugs* **1986**, *32*, 114–129.
(11) Hibert, M. F.; Gittos, M. W.; Middlemiss, D. N.; Mir, A. K.; Fozard, J. R. Graphics Computer- Aided Receptor Mapping as a Predictive Tool for Drug Design: Development of Potent, Selective, and Stereospecivic Ligands for the 5-HT_{1A}. *J. Med. Chem.* **1988**, *31*, 1087–1093.

(12) Hibert, M. F.; McDermott, L.; Middlemiss, D. N.; Mir, A. K.; Fozard, J. R. Radioligand Binding Study of a Series of 5-HT_{1A} Receptor Agonists and Definition of a Steric Model of this Site. *J. Med. Chem.* **1989**, *24*, 31–37.
(13) Sleight, A.; Peroutka, S. J. Identification of 5-Hydroxytryptamine$_{1A}$ Receptor Agents Using a Composite Database Screening. *Naunyn-Schmiedeberg's Arch. Pharmacol.* **1991**, *343*, 109–116.
(14) Agarwal, A.; Taylor, E. W. 3-D QSAR for Intrinsic Activity of 5-HT_{1A} Receptor Ligands by the Method of Comparative Molecular Field Analysis. *J. Comput. Chem.* **1993**, *14*, 237–245.
(15) Mellin, C.; Vallagarda, J.; Nelson, D. L.; Bjork, L.; Yu, H.; Anden, N. E.; Csoregh, I.; Crridsson, L. E.; Hackell, U. A 3-D model for 5-HT_{1A} Receptor Agonists Based on Stereoselective Methylsubstituted and Conformationally Restricted Analogues of 5-Hydroxy-2-(di-n-propylamino)tetralin. *J. Med. Chem.* **1991**, *34*, 497–510.
(16) Vallagarda, J.; Arvidsson, L. E.; Svensson, B. E.; Fowler, C. J.; Hacksell, U. Phenolic Derivatives of 1,2-Methano-N,N-dipropyl-1,2,3,4-tetrahydronaphth-2-ylamine. Structural Hybrids of 2-Aminotetralin- and Phenylcyclopropylamine-Derived 5-HT_{1A}-Receptor Agonists. *Eur. J. Med. Chem.* **1993**, *28*, 399–406.
(17) Hjorth, S.; Carlsson, A. Buspirone: Effects on Central Monoaminergic Transmission-Possible Relevance to Animal Experimental and Clinical Findings. *Eur. J. Pharmacol.* **1982**, *83*, 299–304.
(18) Andronati, S. A.; Varava, V. M.; Soboleva, S. G.; Korneev, A. Y.; Voronina, T. A.; Seredenin, S. B. 1-Phenyl-4-[4-(N-Naphtalimido)Butyl]Piperazin- New Ligand of Serotonin Receptors. *Dokl. Akad. Nauk.* **1992**, *327*, 341–344.
(19) Cybulski, J.; Chilmonczyk, Z.; Szelejewski, W.; Wojtasiewicz, K.; Wróbel, J. T. An Efficient Synthesis of Buspirone and its Analogues. *Arch. Pharmacol. (Weinheim)* **1992**, *325*, 313–315.
(20) (a) Pol. Pat. Appl. P 299147, 1993. (b) Mos, J.; Olivier, B.; Tulp, Th. M. Ethopharmacological Studies Differentiate the Effects of Various Serotonergic Compounds on Aggression in Rats. *Eur. J. Pharmacol.* **1990**, *183*, 1384.
(21) Yevich, J. P.; Temple, D. L., Jr.; New, J. S.; Taylor, D. P.; Riblet, L. A. Buspirone Analogues. 1. Structure-Activity Relationships in a Series of N-Aryl- and Heteroarylpiperazine Derivatives. *J. Med. Chem.* **1983**, *26*, 194–203.
(22) (a) Allen, F. H.; Bellard, S.; Brice, M. D.; Cartwright, B. A.; Doubleday, A.; Higgs, H.; Hummelink, T.; Hummelink-Peters, B. G.; Kennard, O.; Motherwell, W. D. S.; Rodgers, J. R.; Watson, D. G. The Cambrigde Crystallographic Data Centre: Computer-Based Search, Retrieval, Analysis and Display of Information. *Acta Crystallogr.* **1979**, *B35*, 2331–2339. (b) *CSD System Documentation*; Cambridge Crystallographic Data Centre: Cambridge, U.K., 1992.
(23) *Kuma KM-4 Software User's Guide. Ver. 3.1*; Kuma Diffraction: Wrocław, Poland, 1989.
(24) Sheldrick, G. M. *SHELXS-86: Program for crystal structure determination*; University of Göttingen: Germany, 1986.
(25) (a) Sheldrick, G. M. *SHELXTL/PC User's Manual*; Siemens Analytical X-ray Instruments Inc.: Madison, WI, 1991. (b) Sheldrick, G. M. *SHELXL-93: Program for the refinement of crystal structures from diffraction data*; University of Göttingen: Germany, 1993.
(26) Dewar, M. J. S.; Zoebisch, E. G.; Healy, E. F.; Stewart, J. J. P. AM1; A New General Purpose Quantum Mechanical Molecular Model. *J. Am. Chem. Soc.* **1985**, *107*, 3902–3909.
(27) Frish, M. J.; Head-Gordon, M.; Trucks, G. W.; Foresman, J. B.; Schlegel, H. B.; Raghavachari, K.; Robb, M. A.; Binkley, J. S.; Gonzalez, C.; Defrees, D. J.; Fox, D. J.; Whiteside, R. A.; Seeger, R.; Melius, C. F.; Baker, J.; Martin, R. L.; Kahn, L. R.; Stewart, J. J. P.; Topiol, S.; Polple, J. A. *Gaussian 90*; Gaussian Inc.: Pittsburgh, PA, 1990.
(28) Richards, W. G. *Quantum Pharmacology*; Butterworths & Co.: London, 1993; Chapter 16, pp 189–202.
(29) Baginski, M.; Piela, L. Theoretical comparison of Conformational Properties of Molecules. Conformational Probability Maps and Similarity index. *J. Comput. Chem.* **1993**, *14*, 314–328.
(30) Naray-Szabo, G. Electrostatic Complementarity in Drug Design. The Average Molecular Electrostatic Field as a QSAR Descriptor. In *Trends in Medicinal Chemistry '88*; Van der Goot, H., Domany, G., Pallos, L., Timmermann, H., Eds.; Elsevier: Amsterdam, 1989; pp 29–41.
(31) Mazurek, A. P.; Weinstein, H.; Osman, R.; Topiol, S.; Ebersole, B. J. Theoretical and Experimental Studies of Drug-Receptor Interactions: Determinants for Recognition of 5-Hydroxytryptamine Analogs. *Int. J. Quant. Chem. Quant. Biol. Symp.* **1984**, *11*, 183.
(32) Weinstein, H.; Osman, R.; Mazurek, A. P. Simulation of Molecular Stereoelectronic Mechanism for the Interaction of Hallucinogens and Indole Derivatives at 5-HT Receptors. In *Steric Aspects of Biomolecular Interactions*; Naray-Szabo, G., Simon, K., Eds.; CRC Press: Boca Raton, FL, 1987; pp 199–210.
(33) Kalinowski, H.-O.; Berger, S.; Braun, S. Die Chemische Verschiebung. In *^{13}C-NMR-Spektroskopie*, 1st ed.; Georg Thieme Verlag: Stuttgart, 1984; pp 106–114.
(34) Weinstein, H.; Osman, R.; Green, J. P.; Topiol, S. Electrostatic Potentials as Descriptors of Molecular Reactivity: The Basis for Some Succesful Predictions of Biological Activity. In *Chemical Applications of Atomic and Molecular Electrostatic Potentials*; Politzer, P., Truhlar, D. G., Eds.; Plenum Press: New York, 1981; pp 309–334.
(35) Dixon, D. A.; Komornicki, A. Ab Initio Conformational Analysis of Cyclohexane. *J. Phys. Chem.* **1990**, *94*, 5630–5636.
(36) Humblet, C.; Marshall, G. R. Pharmacophore Identification and Receptor Mapping. In *Annnual Reports in Medicinal Chemistry*; Academic Press Inc.: New York, 1980; Vol. 15, pp 267–276.
(37) Mokrosz, J. L.; Pietrasiewicz, M.; Duszyńska, B.; Cegła, M. T. Structure-Activity Relationship Studies of Central Nervous System Agents. 5. Effect of the Hydrocarbon Chain on the Affinity of 4-Substituted 1-(3-Chlorophenyl)piperazines for 5-HT_{1A} Receptor Site. *J. Med. Chem.* **1992**, *35*, 2369–2374.
(38) Gordon, H. L.; Jarrel, H. C.; Szabo, A. G.; Willis, K. J.; Somorjai, R. L. Molecular Dynamics Simulations of the Conformational Dynamics of Tryptophan. *J. Phys. Chem.* **1992**, *96*, 1915–1921.
(39) Henderson, R.; Baldwin, J. M.; Ceska, T. A.; Zemlin, F.; Beckmann, E.; Downing, K. H. Model for the Structure of Bacteriorhodopsin Based on High-Resolution Electron Cryomicroscopy. *J. Mol. Biol.* **1990**, *213*, 899–929.
(40) Henderson, R.; Unwin, P. N. T. Three-Dimensional Model of Purple Membrane Obtained by Electron Microscopy. *Nature* **1975**, *257*, 28–32.
(41) Subramanian, S.; Gerstein, M.; Oesterhelt, D.; Henderson, R. Electron Diffraction Analysis of Structural Changes in the Photocycle of Bacteriorhodopsin. *EMBO J.* **1993**, *12*, 1–9.
(42) Shih, J. C.; Yang, W.; Chen, K.; Gallaher, T. Molecular Biology of Serotonin (5-HT) Receptors. *Pharmacol. Biochem. Behav.* **1991**, *40*, 1053–1058.
(43) Hibert, M. F.; Trumpp-Kallmeyer, S.; Bruinvels, A.; Hoflack, J. Three-Dimensional Models of Neurotransmitter G-Binding Protein-Coupled Receptors. *Mol. Pharmacol.* **1991**, *40*, 8–15.

JM9404702